Adiabatic-impulse approximation in the non-Hermitian Landau-Zener model

Xianqi Tong [1], Gao Xianlong [2,*] and Su-peng Kou[1,†]

[1]*Department of Physics, Beijing Normal University, Beijing 100000, People's Republic of China*
[2]*Department of Physics, Zhejiang Normal University, Jinhua 321004, People's Republic of China*

In the non-Hermitian Landau-Zener models, we investigate the dynamical transition both in parity-time symmetric and symmetry-broken regimes. Taking into account the complex nature of the energy of the non-Hermitian systems, the absolute value of the gap was used to determine the relaxation rate of the system. To show the dynamics of the phase transitions, the relative population is used to estimate the topological defect density in nonequilibrium phase transitions, rather than the excitations in the corresponding Hermitian systems. The result shows that the adiabatic-impulse approximation, which is fundamental to the Kibble-Zurek mechanism, may be adapted to the parity-time symmetric non-Hermitian Landau-Zener models to examine the dynamics near the critical point. The most basic non-Hermitian two-level models with an exact solution exhibiting the Kibble-Zurek mechanism are presented. It would be interesting to extend this scenario to quantum many-body models, such as the quantum phase transition in the Ising model.

I. INTRODUCTION

A two-level quantum system exhibiting either an avoided or a level crossing plays an essential role in the quantum adiabatic dynamics. The transition probability is usually captured by the Landau-Zener (LZ) theory [1,2] as the control parameter changes with time. Usually, the quantum two-level system provides not only qualitative but also quantitative descriptions of the system properties. It has become the standard theory for investigating many physical systems, e.g., the smallest quantum magnets and Fe_8 clusters cooled below 0.36 K are successful described by the LZ model [2,3].

In many cases, the relevant parameters (i.e., the energy gap between the two levels in time) have the potential to be more general than the original LZ process. This motivates us to extend the level-crossing dynamics to level coalescence and various power-law dependencies in this paper. By appropriately varying the external parameters driving the LZ transition, these LZ models can be experimentally realized in polarization optics [4], adiabatic quantum computing [5,6], and non-Hermitian (NH) photonic Lieb lattices [7–9].

Fundamental axioms of quantum mechanics impose the Hermitian nature on the Hamiltonian. However, recent developments have shown the emergence of rich features for NH Hamiltonians describing intrinsic nonunitary dynamics [10–14], which have also been recently realized experimentally [15–17]. Although the eigenvalues of the NH Hamiltonians can still be interpreted in terms of energy bands [18,19], the significance of their eigenvectors can no longer be handled by conventional methods because they are not orthogonal and thus already possess limited overlap without any

additional perturbations [20–25]. In this context, the exceptional points [26–31] (EP) are particularly important, where the complex spectra become gapless. These can be seen as the NH counterparts of the conventional quantum critical points [32–34]. In the EP, two (or more) complex eigenvalues and eigenstates coalesce and then no longer form a complete basis [35–37]. The main purpose of this article is to study the linear quenching dynamics near the critical point, captured by the Kibble-Zurek (KZ) mechanism [27,28,38–44].

In this context, we present a successful combination of the KZ theory of topological defect production [45–47] and the quantum theory of the parity-time (PT) symmetric non-Hermitian Landau-Zener (NHLZ) model [48–51]. Both theories play a prominent role in contemporary physics. The KZ theory predicts the production of topological defects (vortexes, strings) in the course of nonequilibrium phase transitions [17,52–59]. This prediction applies to phase transitions in liquid ^{4}He and ^{3}He, liquid crystals, superconductors, ultracold atoms in optical lattices [60–62], and even to cosmological phase transitions in the early universe [63,64]. However, to the best of our knowledge, the KZ mechanism has not yet been considered in the simplest NH two-level model.

This paper mainly focuses on the dynamical evolution of the PT-symmetric NHLZ model, including adiabatic and impulse regimes during the slow quench of a system parameter. The NHLZ model exhibits a real-to-complex spectral transition, commonly referred to as the PT transition. In the PT-symmetric regime, the eigenvalues are real, ensuring that the probability is conserved. When the energy gap is large enough away from the EP, the adiabatic theorem ensures that a system prepared in an eigenstate remains in an instantaneous eigenstate. This is in contrast to diabatic evolutions induced by a very fast parameter change. It can be seen that the evolution process of the PT-symmetric regime is almost the same as that of the Hermitian system [46]. Attempts to simplify the entire

*Corresponding author: gaoxl@zjnu.edu.cn
†Corresponding author: spkou@bnu.edu.cn

evolution with the adiabatic-impulse (AI) approximation are more involved in the PT-symmetry broken regime where the eigenvalues are complex conjugates. The AI approach has its origins in the KZ theory of classical nonequilibrium phase transitions [65–67]. Furthermore, the probability is no longer conserved because there is an exponential growing and an exponential decaying energy level, and only the exponential growing state is left under the adiabatic evolution. Thus, the adiabatic conditions of the NH system are modified [68–70]. Near the EP, however, due to the reciprocal of the absolute value of the energy gap being greater than the change of the parameters, the dynamics cannot be adiabatic, and the system gets excited. Then, since the probability of the system is not conserved during the evolution, the relative occupation is proposed to calculate the excitation rather than the projection of the excited state. This scenario is captured by the AI approximation. Finally, we also give nontrivial diabatic solutions for the NHLZ model, successfully obtaining the theoretical free parameters in the AI approximation.

In this paper, we demonstrate and discuss the AI approximation from the simplest NH two-level LZ model in two separate sections. Section II presents the AI approximation in the PT-symmetric region and the precise solutions to the two quenching processes: $\gamma \in (-\infty, -\gamma_{EP})$, and (γ_{EP}, ∞), where γ_{EP} represents EP. In Sec. III, we will examine the AI approximation solution of the PT-symmetric broken regime under various initial conditions. In Appendix A, we discuss the exact diabatic solution of the NH Landau-Zener-like problem. Details of the analytic calculations for the exact solutions in the PT-symmetric regimes are presented in Appendix B.

II. PT-SYMMETRIC REGIME

The PT-symmetric NHLZ model we consider is

$$H(t) = \frac{1}{2} \begin{pmatrix} (-1)^n \gamma & \nu \\ \nu(1-\delta) & (-1)^{n+1}\gamma \end{pmatrix}, \quad (1)$$

where $\gamma = \Delta t$ is time-dependent and Δ is time-independent constant. In this section, we take $n = 0$. The system experiences the adiabatic time evolution when $\Delta \to 0$, and $\Delta \to \infty$ means diabatic evolution. In this model, ν and $\delta > 0$ are constant parameters. We set $\nu = 1$ as an energy unit without changing the results. The eigenvalues are $E_s = \pm\frac{1}{2}\sqrt{\gamma^2 + 1 - \delta}$.

For a NH Hamiltonian H, let $\langle i^L|$ denote the ith left eigenstate with (generally complex) eigenenergy E_i, i.e., $\langle i^L|H = \langle i^L|E_i$. Note that the jth right eigenvector $|j^R\rangle$ satisfies $H|j^R\rangle = E_j|j^R\rangle$. Two equations satisfy the biorthonormal relation $\langle i^L|j^R\rangle = \delta_{ij}$.

At any instantaneous time, the right eigenstates of this Hamiltonian can be expressed in the time-independent basis $|1\rangle$ and $|2\rangle$. The ground state $|\downarrow (t)^R\rangle$ and the excited state $|\uparrow (t)^R\rangle$ are given by the following equation:

$$\begin{bmatrix} |\uparrow (t)^R\rangle \\ |\downarrow (t)^R\rangle \end{bmatrix} = \begin{pmatrix} -\frac{i}{\sqrt{\delta-1}}\cosh\frac{\theta}{2} & i\sinh\frac{\theta}{2} \\ -\frac{1}{\sqrt{\delta-1}}\sinh\frac{\theta}{2} & \cosh\frac{\theta}{2} \end{pmatrix} \begin{bmatrix} |1\rangle \\ |2\rangle \end{bmatrix}, \quad (2)$$

where $\cosh\theta = \epsilon/\sqrt{\epsilon^2-1}$, $\sinh\theta = 1/\sqrt{\epsilon^2-1}$, $\epsilon = \gamma/\nu\sqrt{\delta-1}$, $\theta \in [0, \pi]$. If θ is complex, the Hamiltonian's PT symmetry is broken, which is considered in Sec. III.
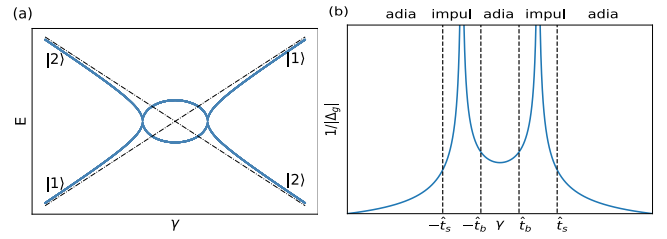

FIG. 1. (a) The energy dispersion relation of the quantum system as a function of γ described in Eq. (1) with $\nu = 1$. Note the level cross occurs at EP $\gamma_{EP} = \pm\sqrt{\delta-1}$ and the asymptotic form of eigenstates is denoted by $|1\rangle$ and $|2\rangle$. The dash-dotted line is for the dispersion relation of the Hamiltonian (1) with $\nu = 0$. (b) The inverse of the energy gap as a function of γ in the NHLZ model. The four dashed lines correspond to the instants $\pm\hat{t}_s$ in the PT-symmetric and $\pm\hat{t}_b$ in the PT-symmetric broken regimes, which separate the adiabatic and impulse regimes.

The energy dispersion of the system is depicted in Fig. 1(a). The energy gap is $\Delta_g = \sqrt{\gamma^2 + \nu^2(1-\delta)}$. Provided that the band gap is sufficiently large, the system is in the adiabatic regime, whereas when the gap is small it undergoes an impulsive time evolution as illustrated in Fig. 1(b). Here, $\pm\hat{t}_s$ and $\pm\hat{t}_b$ represent the instants at which the PT-symmetric and PT-broken regimes switch from adiabatic to impulse, respectively. It can be seen that the energy gap $\Delta_g = 0$ at the EP ($\gamma = |\gamma_{EP}| = \nu\sqrt{\delta-1}$ and $|t_{EP}| = \nu\sqrt{\delta-1}/\tau_Q|\gamma_{EP}|$), which is accompanied by the coalescing of the eigenvalues and eigenstates.

We introduce the density of topological defects in the NHLZ model as follows. Suppose the state $|1^R\rangle$ is the eigenstate of arbitrary NH operator $\hat{O}$: $\hat{O}|1^R\rangle = n|1^R\rangle$ (n is a constant), while the state $|2^R\rangle$ always corresponds to the 0 eigenvalue, i.e., $\hat{O}|2^R\rangle = 0|2^R\rangle$. For any normalized state, it can be written as $|\Psi\rangle = a|1^R\rangle + b|2^R\rangle$ ($|a|^2 + |b|^2 = 1$, $\langle i^L|j^R\rangle = \delta_{ij}$ in the PT-symmetric regime). The unit density defect is determined by the projected value of the operator $\hat{O}$, $\langle\hat{O}\rangle_p = |\langle 1^L|\hat{O}|\Psi\rangle/n|^2 = |\langle 1^L|\Psi\rangle|^2$. But for the nonunitary evolution in the PT-symmetry broken regime, the probability of time evolution state in the instantaneous states is not conserved, i.e., $|a|^2 + |b|^2 \neq 1$. Then, $\langle\hat{O}\rangle_p$ is replaced with the relative occupation as

$$\mathcal{D}_r = \frac{|\langle 1^L|\Psi\rangle|^2}{|\langle 1^L|\Psi\rangle|^2 + |\langle 2^L|\Psi\rangle|^2}, \quad (3)$$

where $\langle n^L|$ is the nth left eigenstate. However, when we discuss only the PT-symmetric regime, where $|\langle 1^L|\Psi\rangle|^2 + |\langle 2^L|\Psi\rangle|^2 = 1$, then $\mathcal{D}_r$ returns back to the Hermitian case, i.e., $\mathcal{D}_r = \langle\hat{O}\rangle_p$.

Suppose the system evolves adiabatically from the ground state of (1) at $t \to -\infty$ to the ground state across the EP. Then, the state of the system will go from a density-free phase to a density-defected one, that is, the system undergoes a phase transition from $|1^R\rangle$ to $|2^R\rangle$. If the time evolution fails to be adiabatic, which is usually the case, then the state at the end is a superposition of states $|1^R\rangle$ and $|2^R\rangle$, so the excitation probability of the operator $\hat{O}$ is nonzero. In this

section, we will demonstrate that the KZ theory can predict the topological density (3) in the NHLZ system.

Consider the dynamics of the LZ model described by the time-dependent Schrödinger equation $i\frac{d}{dt}|\Psi\rangle = H(t)|\Psi\rangle$, where $H(t)$ is given in Eq. (1). When the whole evolution begins at time $t_i \to -\infty$, the initial state is chosen to be the ground state $|\phi_G(t_i)\rangle$, and remains the corresponding instantaneous eigenstate when $t_f \to -t_{EP}$ on the negative half-axis of the time axis. Since the eigenvalues coalesce at EP, no matter how slowly the parameters are driven, it is impossible for the quantum system of a state to evolve adiabatically close to the critical point. The goal of this paper is to quantify this inevitable excitation level in NH systems.

The essence of the KZ mechanism is to simplify the system's dynamics by assuming that the evolution of the system is either adiabatic or diabatic. That is, the quenching process is split into the impulse regime near the EP, where the state is changeless, and the quasiadiabatic regime far from the EP, where the state can adjust to the changes in the parameter. This is the key concept from Zurek [65–67], and the transition from the adiabatic to impulse region is determined by the relevant time scale. In addition, the relevant time scale is proportional to the reciprocal of the energy gap, which is small when the parameter is far from the EP and relatively large in the impulse regime. The adiabatic theorem states that the system will evolve from the ground state and stays in the ground state as long as the reciprocal of the gap is large enough. This demonstrates clearly that, under the adiabatic evolution regime, which can be viewed as the corresponding relaxation time scale defined above, the reciprocal of the gap must be large, $\tau = 1/\sqrt{\gamma^2 + \nu^2(1-\delta)}$. The dimensionless distance $\epsilon = \Delta t/(\nu\sqrt{\delta-1})$ of the system from the exceptional point is equivalent to the relative temperature. The quench time is $\tau_Q = \nu\sqrt{\delta-1}/\Delta \equiv 1/(\tau_0\Delta)$, where $\tau_0 = 1/\nu\sqrt{\delta-1}$ is a time dimensionless constant. Thus, the analogy of the relaxation time scale, relative temperature, and quench time scale are established. Finally, the relaxation time can be written as

$$\tau = \frac{\tau_0}{\sqrt{\epsilon^2 - 1}}, \quad \epsilon = \frac{t}{\tau_Q}. \quad (4)$$

In the limit $|\epsilon| \gg 1$, the relaxation time $\tau \approx \tau_0/|\epsilon|$ will be the same as the theory of topological defect density in liquid ^{4}He [65–67], which will be discussed in details below.

The energies of the system in this section are real at the beginning of the evolution, and the energy gap is large enough so that the states of the system evolve adiabatically. On the contrary, when the time-dependent parameter of the Hamiltonian is gradually approaching an exceptional point, the time-evolved state can not follow the change of the parameter of the Hamiltonian. The evolved state becomes an impulse near the EP. Under the AI approximation, the whole dynamic process is described by the KZ mechanism. So, the whole evolution process can be divided into two different regimes: $t \in (-\infty, -\hat{t})$ and $t \in [-\hat{t}, -t_{EP}]$. In the PT-symmetric regime

$$t \in (-\infty, -\hat{t}) : |\Psi(t)\rangle \approx (\text{phase factor}) |\phi_G(t)\rangle,$$
$$t \in [-\hat{t}, -t_{EP}] : |\Psi(t)\rangle \approx (\text{phase factor})|\phi_G(-\hat{t})\rangle, \quad (5)$$

which is the same for the evolution $t \in [\gamma_{EP}, +\infty)$, because the energy spectrum is real and symmetric on both sides when $|\gamma| > \gamma_{EP}$ ($\gamma_{EP} = \tau_Q t_{EP}$). In Hermitian systems, there are also two regions: A, when $t \in [-\infty, -\hat{t}]$ the wave function is an instantaneous ground state $|\phi_G(t)\rangle$ of the Hamiltonian in the adiabatic regime; B, when $t \in [-\hat{t}, \hat{t}]$ the wave function is in an impulse regime and is essentially unchanged from $-\hat{t}$. At the PT-symmetric regime, $t < -\hat{t}$ (or $t > \hat{t}$) equal to A and $t \in [-\hat{t}, -t_{EP}]$ (or $t \in [t_{EP}, \hat{t}]$) equals to B. The difference, however, is that the impulse regime in a non-Hermitian system is separated by the EP. Since at this point the instantaneous eigenstate coalesces with the other, the time-dependent wave function that passes through the EP has the same population for both instantaneous eigenstates. We conclude that the KZ mechanism defined by the biorthogonal basis in the PT-symmetric regime is basically the same as that in the Hermitian system.

According to Eq. (5), the state will be impulsed in the regime near the EP that only has a different phase factor. When the energy gap away from the EP is large, the state can evolve adiabatically over time. It can be considered the instantaneous eigenstate of the Hamiltonian with a different phase factor. Clearly, the process will revert to adiabatic evolution once the real energy gap becomes large enough. The assumption behind Eq. (5) is based on how well the KZ mechanism works in the NHLZ model.

However, the determination of the density defects still needs to get the instants $\pm\hat{t}$. It was first calculated by Zurek in the paper on classical phase transition [65–67],

$$\tau(\hat{t}) = \alpha\hat{t}, \quad (6)$$

where $\alpha = O(1)$ is a constant *independent* of τ_Q [45,46]. In the PT-symmetric regime, by substituting Eq. (4) into Eq. (6), we get the solution of dimensionless distance ϵ_s,

$$\hat{\epsilon}_s = \epsilon_s(\hat{t}) = \frac{1}{\sqrt{2}}\sqrt{\sqrt{1 + \frac{4}{x_\alpha^2}} + 1}, \quad x_\alpha = \alpha\frac{\tau_Q}{\tau_0}. \quad (7)$$

For fast transition, i.e., $x_\alpha \to 0$, we get $\hat{t} = \sqrt{\tau_0\tau_Q/\alpha}$. In this paper, we obtain the analytical solution of α. The specific example in Appendix A illustrates this approach. The time-dependent Schrödinger equation can be solved exactly in the diabatic limit ($x_\alpha \to 0$) if one looks at the lowest nontrivial terms in the expression for the excitation amplitudes. But getting an exact solution is very complicated. After obtaining α in the way described by Appendix A, the whole AI approximation is complete in the sense that there are no free parameters, so its prediction can be strictly checked by comparison with the diabatic solution.

Since there are two PT-symmetric regimes separated by instants $\pm\hat{t}_s$, we consistently denote two cases when the system evolves from $t < -t_{EP}, t > t_{EP}$ by (i), (ii), which are the same as (i), (ii) in Appendices A and B.

(i) The first case considered is completely in the PT-symmetric region. The initial state $|\Psi(t_i)\rangle$ is set to be the ground state $|\uparrow (t_i)^R\rangle$, and the initial evolution point is away from the EP, i.e., from $-\infty$ to $-\gamma_{EP}$. This implies that in the NH system, the left eigenstate is used to determine the excited state occupation rather than the right eigenstate in the
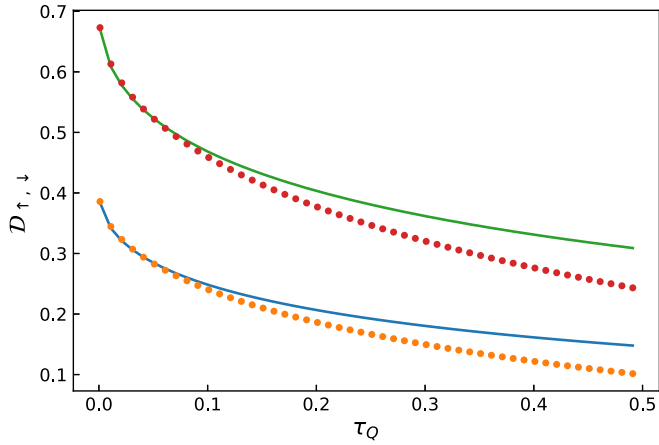
FIG. 2. Transition probability as a function of τ_Q in the PT-symmetric regime for the excitation probability $\mathcal{D}_\downarrow$ (lower curves), and for the $\mathcal{D}_\uparrow$ (upper curves). Solid lines represent the results from the AI approximation (8) and (12). The dotted lines represent the exact solution by substituting the time-dependent wave functions obtained from (B6) and (B7) into (8) and (12). The lower (upper) curves correspond to $\theta_0 = 0.01\pi$ (0.50π) with $\alpha = \frac{\pi}{4}$.

Hermitian system,

$$
\begin{aligned}
\mathcal{D}_\downarrow &= |\langle \downarrow (t_f)^L \mid \widetilde{\Psi}(t_f)\rangle|^2 \approx |\langle \downarrow (t_f)^L \mid \widetilde{\Psi}(-\hat{t})\rangle|^2 \\
&= |\langle \downarrow (-t_n)^L \mid \uparrow (-\hat{t})^R\rangle|^2 \\
&= \tfrac{1}{2}\cosh\theta_0\sqrt{P(x_\alpha)/2} + \tfrac{1}{2}\sinh\theta_0\sqrt{P(x_\alpha)/2 - 1} - \tfrac{1}{2},
\end{aligned}
\tag{8}
$$

where $t_n > 0$ is a point near the EP and $\theta_0 = \operatorname{arctanh}(\tau_Q/t_i) \in [-\pi, \pi]$ measures the distance between the start or end point of the time evolution and the EP, $P(x_\alpha) = 2 + x_\alpha^2 + x_\alpha\sqrt{4 + x_\alpha^2}$, and the $|\widetilde{\Psi}(t_f)\rangle$ is the normalized time-dependent state. During the whole evolution of the NH system, we normalize the wave function at every step dt.

Furthermore, the case of pass over EP is not considered. When the two eigenvectors merge, it is not possible to infer from which of the two states of the system started. Even at the adiabatic limit ($\tau_Q \to \infty$), the density of defects ($\mathcal{D}_\downarrow$) of the final state at the EP is almost the same.

For fast transitions $\tau_Q \to 0$, the excitation probability $\mathcal{D}_\downarrow$ is expanded into a series as below

$$
\begin{aligned}
\mathcal{D}_\downarrow &= \sinh^2\left(\frac{\theta_0}{2}\right) + \frac{1}{2}\sinh(\theta_0)\sqrt{x_\alpha} \\
&\quad + \frac{1}{4}\cosh(\theta_0)x_\alpha + O(x_\alpha^{3/2}).
\end{aligned}
\tag{9}
$$

Here $\theta_0 = -\operatorname{arccoth}(6/5)$, so $\sinh(\theta_0) = -5/\sqrt{11}$ and $\cosh(\theta_0) = 6/\sqrt{11}$. By plugging these values, one can write Eq. (9) as

$$
\mathcal{D}_\downarrow = \sinh^2\left(\frac{\log(11)}{4}\right) - \frac{5\sqrt{x_\alpha}}{2\sqrt{11}} + \frac{3x_\alpha}{2\sqrt{11}} + O(x_\alpha^{3/2}),
\tag{10}
$$

which is plotted as a function of τ_Q in Fig. 2. It turns out that α can be obtained by looking at the diabatic excitation probability. The exact expression and calculation for α can be

found in Appendix A. Substituting $\eta = 1/2$ into Eq. (A6), to the lowest nontrivial order one gets

$$
P_\downarrow = -\frac{1}{2} + \frac{1}{2}\cosh\left(\frac{\log(11)}{2}\right) - \frac{5\sqrt{\frac{\pi}{4}\tau_Q}}{2\sqrt{11}},
\tag{11}
$$

where $P_\downarrow$ denotes diabatic approximation, which implies the exact expression of $\alpha = \frac{\pi}{4}$.

(ii) For the second case, we begin with the ground state at $t_i = \tau_Q/\tanh(\pi/2)$ and end at $t_f \to \infty$. As discussed in Eq. (8), the AI approximation can directly generate the predictions, most notably the probability of finding the system in an excited state is

$$
\begin{aligned}
\mathcal{D}_\uparrow &= |\langle \uparrow (t_f)^L \mid \widetilde{\Psi}(t_f)\rangle|^2 \\
&\approx |\langle \uparrow (\hat{t})^L \mid \uparrow (t_i)^R\rangle|^2 \\
&= \tfrac{1}{2}\cosh\theta_0\sqrt{P(x_\alpha)/2} - \tfrac{1}{2}\sinh\theta_0\sqrt{P(x_\alpha)/2 - 1} - \tfrac{1}{2}.
\end{aligned}
\tag{12}
$$

Here, we assumed that

$$
\begin{aligned}
|\langle \uparrow (t_f)^L \mid \widetilde{\Psi}(t_f)\rangle|^2 &\approx |\langle \uparrow (\hat{t})^L \mid \widetilde{\Psi}(\hat{t})\rangle|^2 \\
&\approx |\langle \uparrow (\hat{t})^L \mid \widetilde{\Psi}(t_i)\rangle|^2 \\
&= |\langle \uparrow (\hat{t})^L \mid \downarrow (t_i)^R\rangle|^2.
\end{aligned}
\tag{13}
$$

For a fast transformation $\tau_Q \to 0$, we can expand $\mathcal{D}_\uparrow$ into a series

$$
\begin{aligned}
\mathcal{D}_\uparrow &= \sinh^2\left(\frac{\theta_0}{2}\right) - \frac{1}{2}\sinh(\theta_0)\sqrt{x_\alpha} \\
&\quad + \frac{1}{4}\cosh(\theta_0)x_\alpha + O(x_\alpha^{3/2}),
\end{aligned}
\tag{14}
$$

where $\theta_0 \to \pi/2$. The determination of the constant α is presented in Appendix A. By substituting $\eta = 1/2$ into Eq. (A9), we can get $\alpha = \pi/4$. That is, to obtain the constant α, this method of combining AI approximation and diabatic solution prediction leads to completely satisfactory results that are much easier and more elementary than the determination of the exact LZ solution [1]. A comparison between the AI prediction for $\alpha = \pi/4$ and the exact solution is shown in Fig. 2. Given that the initial state is prepared far away or in the vicinity of the EP, the system is within the freezing regime of the time interval $[-\hat{t}, -t_{EP}]$ or $[t_{EP}, \hat{t}]$, as shown in Fig. 2 and illustrated below.

A comparison of AI approximations in Eq. (8) and Eq. (12) to the exact results performed in Appendix B for $\tau_Q/\tau_0 < 0.15$ and $|\theta_0 - \pi/2| \leqslant \pi/10$ proclaims satisfactory agreement, see Fig. 2. For larger τ_Q or $|\theta_0 - \pi/2|$ the agreement gradually decreases, due to the fact that for the parameter at the start time (end time) $t_i = \tau_Q/\tanh(\theta_0)$ ($t_f = \tau_Q/\tanh(\theta_f)$), maybe outside the impulse regime $[-\hat{t}, -t_{EP}]$ or $[t_{EP}, \hat{t}]$, where the initial assumption is violated. One avoids these problems when $t_i \ll -\hat{t}$ and $|t_f| \ll \hat{t}$, i.e., when the entire evolution of the system is clearly divided into adiabatic and frozen regimes, see Eq. (5).

III. PT-SYMMETRIC BROKEN REGIME

When the evolution is a full NH drive, is it possible to see agreement between precise solutions and AI approximations

in the PT-symmetric broken region? In Hamiltonian (1), we assume $n = 1/2$, so $(-1)^{1/2} = i$ is an imaginary number. It must be remembered that δ should be 0 in the PT-symmetric broken regime. For the PT-symmetric broken regime, we can write the Hamiltonian as

$$H(t) = \frac{1}{2}\begin{pmatrix} i\gamma & v \\ v & -i\gamma \end{pmatrix}, \tag{15}$$

where $\gamma = \Delta t$. Moreover, the quench time $\tau_Q = 1/\Delta\tau_0$ with $\tau_0 = 1/v$. The time-evolving right eigenstates have transformed into the following states:

$$\begin{bmatrix} |\uparrow (t)^R\rangle \\ |\downarrow (t)^R\rangle \end{bmatrix} = \begin{pmatrix} \frac{1}{\sqrt{1-e^{2\beta}}}ie^{\beta} & \frac{1}{\sqrt{1-e^{2\beta}}} \\ \frac{1}{\sqrt{1-e^{-2\beta}}}ie^{-\beta} & \frac{1}{\sqrt{1-e^{-2\beta}}} \end{pmatrix}\begin{bmatrix} |1\rangle \\ |2\rangle \end{bmatrix}, \tag{16}$$

where β is determined by $\sinh\beta = \mathrm{sgn}(\gamma)\sqrt{\gamma^2 - 1}$, $\cosh\beta = |\gamma|$, $\beta \in (-\infty, +\infty)$. This full NH drive is equivalent to quenching the imaginary tachyon mass [15]. The eigenvalues of the Hamiltonian are

$$E_b = \pm\frac{i}{2}\sqrt{\gamma^2 - v^2}. \tag{17}$$

For $|\gamma| > v$, the system is in the PT-symmetric broken regime, where all eigenvalues are imaginary. Otherwise, the eigenvalues are all real when $|\gamma| < v$, i.e., the system is in the PT-symmetric regime.

As the eigenvalues are complex conjugate and there is an exponentially growing state and an exponentially decaying state. Likewise, we assume that time starts from the ground state of $-\infty$ and continues to $-\gamma_{EP}$, or from γ_i to ∞, where γ_i is in the impulse regime on the other side. However, the ground state here refers to the eigenstate corresponding to the positive eigenvalue because γ changes adiabatically. Now the system has enough time to evolve to the exponentially growing state. This state corresponds to the least-dissipative instantaneous eigenstate with the largest imaginary eigenvalue and dominates the adiabatic process. This is unique to the non-Hermitian system, absent from Hermitian dynamics. Thus, the initial state is always chosen to be the least-dissipative eigenstate $|\phi_l(t_i)^R\rangle$. When the time-dependent state evolves to the vicinity of the exceptional point, the state will be excited. In Fig. 3, we plot the density of defects as a function of τ_Q for two different $\alpha_0 = 0.20\pi$ (1.25π). The density of topological defects calculated by the relative population is a function of τ_Q. Surprisingly, we discover that the KZ mechanism is still valid in the PT-symmetric regime and can accurately describe the slow quench dynamics. The KZ mechanism only describes the impulse regime's density when the instantaneous transition rate $\dot{\epsilon}/\epsilon$ is much larger than the energy gap Δ_g, completely different from the Hermitian system [45,46]. Therefore, these two important approximations coming from passing through first adiabatic, then impulse regime in comparison to Eq. (5) can be considered,

$$t \in (-\infty, -\hat{t}) : |\Psi(t)\rangle \approx \text{(phase factor) } |\phi_l(t)^R\rangle,$$

$$t \in [-\hat{t}, -\gamma_{EP}] : |\Psi(t)\rangle \approx \text{(phase factor)}|\phi_l(-\hat{t})^R\rangle. \tag{18}$$

The same holds in the interval $t \in [t_{EP}, \infty)$. Adiabaticity in the Hermitian system means that the probabilities are constant. But in the NH systems, only the least dissipative state can evolve adiabatically because the probabilities on the other
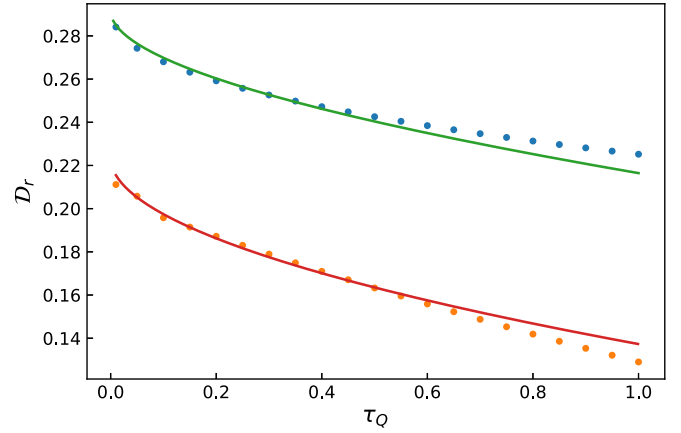

FIG. 3. Relative transition probability as a function of τ_Q in the PT-symmetric broken regime. Solid lines represent the AI approximation from (20) and (23). The lower (upper) curves correspond to $\alpha_0 = 0.20\pi$ (1.25π). Dotted lines represent the numerics by solving Eq. (B9) with the corresponding initial conditions of $\alpha_0 = 0.20\pi$ (1.25π). For all the curves $\alpha = \frac{121}{400}[E_{\frac{1}{2}}(\frac{121}{200})]^2$.

states are suppressed. Nonetheless, the definition remains unchanged in the impulse regions.

However, the eigenvalues are purely imaginary numbers, so the "relaxation time" is not the energy gap of real eigenvalues but rather the absolute value of the imaginary eigenvalue difference,

$$\tau = \frac{\tau_0}{|\sqrt{1 - \epsilon^2}|}, \quad \epsilon = \frac{t}{\tau_Q}, \tag{19}$$

where $\tau_0 = v = 1$. Naturally, after substituting Eq. (19) into Eq. (6), one obtains the dimensionless distance $\hat{\epsilon}_b = \frac{1}{\sqrt{2}}\sqrt{1+\sqrt{1+\frac{4}{x_\alpha^2}}}=\hat{\epsilon}_s$.

Since there are two PT-symmetric broken regimes separated by instants $\pm\hat{t}_b$, we consistently denote the other two cases when the system evolves from $t < -t_{EP}, t > t_{EP}$ by (iii), (iv), which are the same as (iii), (iv) in Appendices A and B.

(iii) For the third case, we examine the situation where the initial state is chosen to the least eigenstate prepared in the impulse area close to the EP, and assume the limits $t_f \to \hat{t}$. Taking the initial state

$$|\Psi(t_i)\rangle = |\uparrow (t_i)^R\rangle = \frac{1}{\sqrt{1 - e^{-2\beta_0}}}ie^{\beta_0}|1\rangle + \frac{1}{\sqrt{1 - e^{-2\beta_0}}}|2\rangle,$$

However, due to the nonunitary time-dependent evolution, $\mathcal{D}_\uparrow$ may be greater than 1. Instead of the $\mathcal{D}_\uparrow$ in Eq. (12), the relative population of the instantaneous eigenstates is proposed to calculate the density [49],

$$\mathcal{D}_r = \frac{|\langle\uparrow (t_f)^L|\tilde{\Psi}(t_f)\rangle|^2}{|\langle\uparrow (t_f)^L|\tilde{\Psi}(t_f)\rangle|^2 + |\langle\downarrow (t_f)^L|\tilde{\Psi}(t_f)\rangle|^2}$$

$$\approx \frac{|\langle\uparrow (\hat{t})^L|\downarrow (t_i)^R\rangle|^2}{|\langle\uparrow (\hat{t})^L|\downarrow (t_i)^R\rangle|^2 + |\langle\downarrow (\hat{t})^L|\downarrow (t_i)^R\rangle|^2}$$

$$= \frac{\sinh(\beta_0)}{2\sqrt{P(x_\alpha)/2 - 1} - \cosh(\beta_0)\sqrt{2P(x_\alpha)}} + \frac{1}{2}, \tag{20}$$

where $\beta_0 = \mathrm{arccosh}|\gamma_i| \in [0, \infty)$ measures the distance of the starting point from the exceptional point, e.g., $\beta_0 = \pi/2$ when evolution starts from a crossing center. Here, we assumed that $|\langle \uparrow (t_f)^L|\tilde{\Psi}(t_f)\rangle|^2 \approx |\langle \uparrow (\hat{t})^L|\tilde{\Psi}(\hat{t})\rangle|^2 \approx |\langle \uparrow (\hat{t})^L|\tilde{\Psi}(t_i)\rangle|^2 = |\langle \uparrow (\hat{t})^L| \downarrow (t_i)^R\rangle|^2$. However, in the PT-symmetric broken phase, it is worth noting that truncation is needed for time t_f to ensure that the probability is not greater than 1, means $\dot{\epsilon}/\epsilon \ll \Delta_g$. It is needed to do truncation in numerical value, and a good agreement between AI approximation and numerics is easily noticed.

AI predictions can be directly compared to accurate results Eq. (A15) after series expansion

$$\mathcal{D}_r = \frac{1}{e^{2\beta_0} + 1} + \frac{\tanh(\beta_0)\mathrm{sech}(\beta_0)}{2}\sqrt{x_\alpha} + O(x_\alpha^{1/2}), \quad (21)$$

where α is easily determined and is presented in Appendix A. By putting $\eta = 1/2$ into Eq. (A15) one can get $\alpha = \frac{121}{400}[E_{\frac{1}{2}}(\frac{121}{200})]^2$, where E_n is the exponential integral function given by $E_n(z) = \int_1^\infty \frac{e^{-zt}}{t^n} dt$.

(iv) The fourth case considered evolves the system to the vicinity of the critical point, $t_f \to -t_n$. The initial condition is starting from the ground state at $t_i \to -\infty$ and assuming that

$$|\langle \downarrow (t_f)^L|\tilde{\Psi}(t_f)\rangle|^2 \approx |\langle \downarrow (-t_n)^L | \tilde{\Psi}(-\hat{t})\rangle|^2$$
$$\approx |\langle \downarrow (-t_n)^L| \downarrow (-\hat{t})^R\rangle|^2, \quad (22)$$

and we obtained

$$\mathcal{D}_r = -\frac{\sinh(\beta_0)}{2\sqrt{P(x_\alpha)/2 - 1} - \cosh(\beta_0)\sqrt{2P(x_\alpha)}} + \frac{1}{2}. \quad (23)$$

The excitation after the expansion equal to

$$\mathcal{D}_r = \frac{1}{e^{2\beta_0} + 1} - \frac{\tanh(\beta_0)\mathrm{sech}(\beta_0)}{2}\sqrt{x_\alpha} + O(x_\alpha^{1/2}), \quad (24)$$

As clear from the above expressions, the exact calculation in Appendix A gives the constant α for the first nontrivial term in Eq. (24), which substituting into Eq. (A16) with $\eta = 1/2$ gives $\alpha = \frac{121}{400}[E_{\frac{1}{2}}(\frac{121}{200})]^2$.

Figure 3 shows a comparison of the Eq. (20) and numerical evolution (B9) with τ_Q. For $\tau_Q/\tau_0 < 1.2$ and $|\beta_0| \leqslant \pi/2$, the two show good agreement. For larger τ_Q, however, the agreement gradually decreases, which we attribute to the fact that the starting time $t_i = \tau_Q \cosh(\beta_0)$ may be beyond the impulse regime $[t_{EP}, \hat{t}]$, or the final point $t_f = \tau_Q \cosh(\beta_f)$ may be less the impulse regime $[-\hat{t}, -t_{EP}]$. So that the assumption that the initial evolution or the end stage is an impulse is violated. To avoid this, the starting point $t_i \ll \hat{t}$ or $t_f \gg -\hat{t}$, i.e., the whole evolution within the two regimes has been described in Eq. (18).

IV. SUMMARY

We have demonstrated that, based on the assumption of the Kibble-Zurek mechanism, the AI approximation can be generalized to provide good quantitative predictions about the adiabatic dynamics of NH two-level Landau-Zener-like systems. The AI approximation is key to the KZ mechanism, as it enables us to calculate the excitations in the frozen region. We use the relative occupation instead of the projections on the exciting eigenstate in the Hermitian system when

the probabilities are not conserved. First, we discuss only the PT-symmetric regimes, where we have found a KZ-like dependence of the topological defect density on the quench rate, which is similar to the Hermitian Landau-Zener model. In addition, the scheme of adiabatic and impulse regimes is basically consistent with the corresponding Hermitian system. Secondly, when the entire evolution is a complete NH drive process, we have found that the reciprocal of the absolute value of the complex energy spectrum can characterize the relaxation time of the system, and it can be used to approximate the transition from adiabatic to freezing. Our results show that the KZ-like mechanism also predicts the density of defects in the diabatic regimes of the PT-symmetric broken regimes.

We expect that the AI approximation can be generalized to arbitrary NH two-level models, many-body models such as the Ising model [54], and even incommensurate models such as the Aubry-André model [55,71–75]. Finally, the results for slow quenching in the vicinity of EP can be verified experimentally, for example, as in cold Fe_8 clusters [2,3], Mach-Zender interferometer [47], and single-photon interferometry [28].

APPENDIX A: EXACT DIABATIC EXPRESSION FOR TRANSITION PROBABILITY

To test the predictions of the AI approximation for a PT-symmetric two-level system different from the Landau-Zener model and determine the exact value of the constant α, we investigate the dynamics induced by the Hamiltonian [46]

$$H(t) = \frac{1}{2}\begin{pmatrix} (-1)^n \mathrm{sgn}(t)\left|\frac{t}{\tau_Q}\right|^{\frac{\eta}{1-\eta}} & 1 \\ 1 - \delta & (-1)^{n+1} \mathrm{sgn}(t)\left|\frac{t}{\tau_Q}\right|^{\frac{\eta}{1-\eta}} \end{pmatrix},$$
$$(A1)$$

where $\eta \in (0, 1)$ are constant [when $\eta = 1/2$, the system is simplified to the NHLZ model (1)]. We propose the lowest order exact formulation of the exciting probability in a class of the NH two-level systems described by the Hamiltonian (A1).

First, when $n = 0, \delta = 2$, the evolution is assumed to occur in the PT-symmetric regimes, e.g., in the interval $|t| > \tau_Q$ when $\eta = 1/2$. Then the time-depended wave function is expressed as

$$|\Psi(t)\rangle = C_1(t)\exp\left(\frac{-i(1-\eta)|t|^{1/(1-\eta)}}{2\tau_Q^{\eta/(1-\eta)}}\right)|1\rangle$$
$$+ C_2(t)\exp\left(\frac{i(1-\eta)|t|^{1/(1-\eta)}}{2\tau_Q^{\eta/(1-\eta)}}\right)|2\rangle, \quad (A2)$$

where the exponential is from $\mp i \int dt \, \text{sgn}(t) |t/\tau_Q|^{\eta/(1-\eta)}/2$. This wave function is reduced to two first-order differential equations concerning $C's$ by the time-dependent Schrödinger equation

$$\dot{C}_1(t) = \frac{1}{2i} \exp\left(\frac{i(1-\eta)|t|^{1/(1-\eta)}}{\tau_Q^{\eta/(1-\eta)}}\right) C_2(t), \quad (A3)$$

$$\dot{C}_2(t) = \frac{1}{2i} k \exp\left(\frac{-i(1-\eta)|t|^{1/(1-\eta)}}{\tau_Q^{\eta/(1-\eta)}}\right) C_1(t). \quad (A4)$$

(i) *Time evolution from the ground state of $t_i \to -\infty$ to $t_f \to -t_n$*. Here t_n means evolution in the vicinity of EP. We want to integrate Eq. (A3) from $-\infty$ to $-t_n$. The initial conditions are $C_1(-\infty) = 1$, $C_2(-\infty) = 0$. Simplification occurs when one assumes a quite fast transition, i.e., $\tau_Q \to 0$. Then obviously $C_1(t) = 1 + O(\tau_Q^\beta)$ with $\beta > 0$. Substituting such $C_1(t)$ into Eq. (A4), we get

$$C_2(-\gamma_n) = \frac{1}{2i} k \tau_Q^\eta \int_{-\infty}^{-\gamma_n} d\gamma \exp\left[-i(1-\eta)|\gamma|^{1/(1-\eta)}\right]$$
$$+ \text{(higher-order terms in } \tau_Q\text{)}, \quad (A5)$$

where $-\gamma_n$ means the point near $-\gamma_{EP}$. $C_1(-\gamma_n) \approx 1$, which after some algebra results in

$$\mathcal{D}_\downarrow = |\langle 2^L|\Psi(t_f)\rangle|^2 = 1 - |\langle 1^L|\Psi(t_f)\rangle|^2$$
$$= -\frac{1}{2} + \frac{1}{2}\cosh\left(\frac{\log(11)}{2}\right) - \frac{5}{2\sqrt{11}}(\alpha\tau_Q)^\eta$$
$$+ \text{(higher-order terms in } \tau_Q\text{)}, \quad (A6)$$

where

$$\alpha = \left(\frac{36}{25}\right)^{1/\eta} \left\{ (1-\eta)^{2\eta}\Gamma(1-\eta)^2 \right.$$
$$\left. \times I_m\left[\left(i\left(-\frac{6}{5}\right)^{\frac{1}{1-\eta}}\right)^{\eta-1}\right]^2 \right\}^{1/\eta}, \quad (A7)$$

here the I_m stands for the imaginary part.

(ii) *Time evolution from the ground state of $t_i \to t_n$ to $+\infty$*. Here the initial function is $\frac{-i}{\sqrt{2}}\sqrt{\frac{\gamma_0}{\sqrt{\gamma_0^2-1}}+1}|1^R\rangle + \frac{i}{\sqrt{2}}\sqrt{\frac{\gamma_0}{\sqrt{\gamma_0^2-1}}+1}|2^R\rangle$. For fast transition one has that $C_1(t) = \frac{-i}{\sqrt{2}}\sqrt{\frac{\gamma_0}{\sqrt{\gamma_0^2-1}}+1} + O(\tau_Q^\beta)$, $C_2(t) = \frac{i}{\sqrt{2}}\sqrt{\frac{\gamma_0}{\sqrt{\gamma_0^2-1}}+1} + O(\tau_Q^\delta)$, where $\beta, \delta > 0$ are constants. Integrating Eq. (A4) from γ_0 to ∞, one gets

$$C_2(+\infty) = \frac{ik\tau_Q^\eta}{2\tanh\frac{\pi}{4}} \int_{\gamma_0}^{+\infty} d\gamma \exp\left[-i(1-\eta)\gamma^{1/(1-\eta)}\right]$$
$$- \frac{i}{\sqrt{2}}\sqrt{\frac{\gamma_0}{\sqrt{\gamma_0^2-1}}+1}$$
$$+ \text{(higher-order terms in } \tau_Q\text{)}, \quad (A8)$$

which makes it easy to show that

$$\mathcal{D}_\uparrow = |\langle 1^L|\Psi(t_f)\rangle|^2 = 1 - |\langle 2^L|\Psi(t_f)\rangle|^2$$
$$= \sinh^2\left(\frac{\log(5)}{4}\right) - \frac{1}{\sqrt{5}}(\alpha\tau_Q)^\eta$$
$$+ \text{(higher-order terms in } \tau_Q\text{)}, \quad (A9)$$

where $\alpha = (1-\eta)^{2\eta}\cos^2(\frac{\pi\eta}{2})\Gamma(1-\eta)^2$.

(iii) *Time evolution from $t \to t_n$ to $t \to t_f$ in the PT-symmetric broken regime*. Because at $t \to \infty$, the positive energy eigenstate will dominate the occupation probability, and the exponential increase of the least dissipative state over time suppresses another eigenstate with negative imaginary energy, so it is required time truncation $t_f \approx \hat{t}$. And we assume that the Hamiltonian is given by Eq. (A1) with $n = 1/2$, $\delta = 0$.

Because the parameter $n = 1/2$, $\delta = 0$ of the Hamiltonian in PT-symmetry broken regime are different from the value of the PT-symmetric phase (1), the wave function is rewritten as

$$|\Psi(t)\rangle = C_1(t) \exp\left(\frac{(1-\eta)|t|^{1/(1-\eta)}}{2\tau_Q^{\eta/(1-\eta)}}\right)|1\rangle$$
$$+ C_2(t) \exp\left(\frac{-(1-\eta)|t|^{1/(1-\eta)}}{2\tau_Q^{\eta/(1-\eta)}}\right)|2\rangle. \quad (A10)$$

Substituting the above wave function into the Schrödinger equation, it can be reduced to

$$\dot{C}_1(t) = \frac{C_2(t)}{2i} \exp\left(\frac{-(1-\eta)|t|^{1/(1-\eta)}}{\tau_Q^{\eta/(1-\eta)}}\right), \quad (A11)$$

$$\dot{C}_2(t) = \frac{C_1(t)}{2i} \exp\left(\frac{(1-\eta)|t|^{1/(1-\eta)}}{\tau_Q^{\eta/(1-\eta)}}\right). \quad (A12)$$

Integration of Eq. (A11) and Eq. (A12) separately gives

$$C_1(\gamma_f) = \frac{\tau_Q^\eta}{2i} i e^{\pi/2} \int_{\gamma_n}^{\gamma_f} d\gamma \exp[-(1-\eta)\gamma^{1/(1-\eta)}] + 1$$
$$+ \text{(high-order terms of } \tau_Q\text{)}, \quad (A13)$$

$$C_2(\gamma_f) = \frac{\tau_Q^\eta}{2i} \int_{\gamma_n}^{\gamma_f} d\gamma \exp[(1-\eta)\gamma^{1/(1-\eta)}] + i e^{\pi/2}$$
$$+ \text{(high-order terms of } \tau_Q\text{)}. \quad (A14)$$

Then the relative occupation leads to the following prediction:

$$\mathcal{D}_r = \frac{|\langle 2^L|\Psi(t_f)\rangle|^2}{|\langle 1^L|\Psi(t_f)\rangle|^2 + |\langle 2^L|\Psi(t_f)\rangle|^2}$$
$$= \frac{1}{12}(6 - \sqrt{11}) + (\alpha\tau_Q)^\eta$$
$$+ \text{(high-order terms of } \tau_Q\text{)}, \quad (A15)$$

where

$$\alpha = \left(\frac{11}{20}\right)^{1/\eta} E_\eta\left(\left(\frac{11}{10}\right)^{\frac{1}{1-\eta}}(1-\eta)\right). \quad (A16)$$

where E is the exponential integral function given by $E_n(z) = \int_1^\infty \frac{e^{-zt}}{t^n} dt$.

(iv) *Time evolution from $t_i \to -\infty$ to $t_f \to -t_n$ in the PT-symmetric broken regime.* To correctly calculate the density of topological defects, we need to introduce the relative population in Eq. (3) instead of projection on excited states in Eq. (8).

Because the unnormalized initial wave function is $(ie^{\pi/2}, 1)$ we have $C_1(\gamma_0) = ie^{\pi/2}$ and $C_2 = 1$. For fast transition, one has that $C_1(t) = ie^{\pi/2} + O(\tau_Q^\beta)$, where $\beta > 0$ is a constant. Integrating Eq. (A11) and Eq. (A12) from $-\infty$ to $-t_n$, one gets

$$C_1(\gamma_f) = \frac{\tau_Q^\eta}{2i} i e^{\pi/2} \int_{-\infty}^{-\gamma_n} d\gamma \exp\left[-(1-\eta)\gamma^{1/(1-\eta)}\right]$$
$$+ \text{(high-order terms of } \tau_Q), \quad \text{(A17)}$$

$$C_2(\gamma_f) = \frac{\tau_Q^\eta}{2i} \int_{-\infty}^{-\gamma_n} d\gamma \exp\left[(1-\eta)\gamma^{1/(1-\eta)}\right] + 1$$
$$+ \text{(high-order terms of } \tau_Q), \quad \text{(A18)}$$

which according to Eq. (3) can easily leads to

$$\mathcal{D}_r = \frac{|\langle 1^L | \Psi(t_f)\rangle|^2}{|\langle 1^L | \Psi(t_f)\rangle|^2 + |\langle 2^L | \Psi(t_f)\rangle|^2}$$
$$= \frac{1}{12}(6 - \sqrt{11}) - (\alpha\tau_Q)^\eta$$
$$+ \text{(high-order terms of } \tau_Q), \quad \text{(A19)}$$

with α is defined in Eq. (A16).

APPENDIX B: EXACT SOLUTIONS OF THE NON-HERMITIAN LANDAU-ZENER SYSTEM

In this section, we present the exact solution to the dynamics of the NH LZ model [1,46,48–50]. The model is similar to Eq. (1), described by the ordinary differential equations for probability amplitudes c_1 and c_2,

$$i\frac{d}{dt}c_1(t) = \frac{1}{2}\gamma(t)c_1(t) + \frac{1}{2}\nu c_2(t),$$
$$i\frac{d}{dt}c_2(t) = \frac{1}{2}\nu k c_1(t) - \frac{1}{2}\gamma(t)c_2(t). \quad \text{(B1)}$$

We can get the second-order equation of $c_2(t)$ by decoupling the above equation by differentiating it again

$$\frac{d^2}{dt^2}c_2(t) + \frac{1}{4}\left(k + \frac{t^2}{\tau_Q^2} - \frac{2i}{\tau_Q}\right)c_2(t) = 0. \quad \text{(B2)}$$

Then a solution with the initial condition $|c_1(t \to -\infty)|^2 = 0$, $|c_2(t \to -\infty)|^2 = 1$ is given by

$$c_2(t) = a D_{-\frac{1}{4}ik\tau_Q - 1}\left(\frac{e^{i\pi/4}t}{\sqrt{\tau_Q}}\right) + b D_{-\frac{1}{4}ik\tau_Q - 1}\left(-\frac{e^{i\pi/4}t}{\sqrt{\tau_Q}}\right), \quad \text{(B3)}$$

the general solution can be expressed in terms of the independent Weber function $D_\nu(z)$, where $\nu = \frac{1}{4}ik\tau_Q$, $z = -\frac{e^{i\pi/4}t}{\sqrt{\tau_Q}}$. Then, the time-dependent wave function can be obtained from

the Schrödinger equation

$$|\Psi(t)\rangle = \frac{2i}{k}\left[\partial_t - \frac{it}{2\tau_Q}\right][aD_{-\nu-1}(iz) + bD_{-\nu-1}(-iz)]|1\rangle$$
$$+ [aD_{-\nu-1}(iz) + bD_{-\nu-1}(-iz)]|2\rangle. \quad \text{(B4)}$$

The constants a and b are as determined from the initial values of $c_1(t_i)$ and $c_2(t_i)$,

$$a = \frac{\Gamma(1-\nu)}{\sqrt{2\pi}}[D_{\nu-1}(-z_i)c_1(t_i) + 2\sqrt{\tau_Q}e^{i\pi/4}D_\nu(-z_i)c_2(t_i)],$$
$$b = \frac{\Gamma(1-\nu)}{\sqrt{2\pi}}[D_{\nu-1}(z_i)c_1(t_i) - 2\sqrt{\tau_Q}e^{i\pi/4}D_\nu(z_i)c_2(t_i)].$$
$$\text{(B5)}$$

(i) *Exact solution to the NHLZ problem when evolution begins at $t_i \to -\infty$, i.e., $|\Psi(-\infty)\rangle \sim |1^R\rangle$.* The Hamiltonian is given by Eq. (B1), together with the $c_2(t)$ and initial condition yields $a = 0$, $b = k\sqrt{\tau_Q}e^{-k\pi\tau_Q/16}/2$. Substituting them into Eq. (B4) results in

$$|\Psi(t)\rangle = e^{i3\pi/4}e^{\frac{-k\pi\tau_Q}{16}}D_{-\frac{1}{4}ik\tau_Q}\left(-\frac{e^{i\pi/4}}{\sqrt{\tau_Q}}t\right)|1\rangle$$
$$+ \frac{k\sqrt{\tau_Q}}{2}e^{-\frac{k\pi\tau_Q}{16}}D_{-\frac{1}{4}ik\tau_Q - 1}\left(-\frac{e^{i\pi/4}}{\sqrt{\tau_Q}}t\right)|2\rangle. \quad \text{(B6)}$$

The density defect can be calculated by the $\mathcal{D}_\uparrow$, which leads to the excitation probability of the system at t_f in the form of Eq. (A6).

(ii) *Exact solution of LZ problem when evolution starts from a ground state at PT-symmetric regime.* From $t_i \to t_n$ to $t_f \to \infty$. Combining the initial condition $c_1(t_i) = \frac{-i}{\sqrt{2}}\sqrt{\frac{\gamma_0}{\sqrt{\gamma_0^2-1}} + 1}$, $c_2(t_i) = \frac{i}{\sqrt{2}}\sqrt{\frac{\gamma_0}{\sqrt{\gamma_0^2-1}} + 1}$ and Eq. (B5), the constants a and b can be obtained

$$a = \frac{1}{c}\left[e^{\frac{i\pi}{4}}\sqrt{\tau_Q}\sinh\left(\frac{\log(21)}{4}\right)D_{\frac{i\tau_Q}{4}-1}\left(-\frac{11}{10}e^{\frac{i\pi}{4}}\sqrt{\tau_Q}\right)\right.$$
$$\left. + 2\cosh\left(\frac{\log(21)}{4}\right)D_{\frac{i\tau_Q}{4}}\left(-\frac{11}{10}e^{\frac{i\pi}{4}}\sqrt{\tau_Q}\right)\right],$$
$$b = \frac{1}{c}\left[2\cosh\left(\frac{\log(21)}{4}\right)D_{\frac{i\tau_Q}{4}}\left(\frac{11}{10}e^{\frac{i\pi}{4}}\sqrt{\tau_Q}\right)\right.$$
$$\left. - e^{\frac{i\pi}{4}}\sqrt{\tau_Q}\sinh\left(\frac{\log(21)}{4}\right)D_{\frac{i\tau_Q}{4}-1}\left(\frac{11}{10}e^{\frac{i\pi}{4}}\sqrt{\tau_Q}\right)\right], \quad \text{(B7)}$$

where

$$c = 2D_{\frac{i\tau_Q}{4}}\left(-\frac{11}{10}e^{\frac{i\pi}{4}}\sqrt{\tau_Q}\right)D_{\frac{i\tau_Q}{4}-1}\left(\frac{11}{10}e^{\frac{i\pi}{4}}\sqrt{\tau_Q}\right)$$
$$+ 2D_{\frac{i\tau_Q}{4}}\left(\frac{11}{10}e^{\frac{i\pi}{4}}\sqrt{\tau_Q}\right)D_{\frac{i\tau_Q}{4}-1}\left(-\frac{11}{10}e^{\frac{i\pi}{4}}\sqrt{\tau_Q}\right). \quad \text{(B8)}$$

From here, it is easy to prove that when $t_f \to \hat{t}$, the modulus of the projection of the system on state $|2^L\rangle$ is equal to Eq. (A9).

However, the PT-symmetric broken regime is too small to observe the adiabatic-impulse transition. The Hamiltonian is replaced by the case of $n = 1/2$, $\delta = 0$ in the Eq. (1), and the

ordinary differential equations are obtained,

$$i\frac{d}{dt}d_1(t) = \frac{1}{2}i\gamma(t)d_1(t) + \frac{1}{2}vd_2(t),$$

$$i\frac{d}{dt}d_2(t) = \frac{1}{2}vd_1(t) - \frac{1}{2}i\gamma(t)d_2(t), \quad \text{(B9)}$$

And the process to get the d_1 and d_2 is the same as the Eq. (B2), but with $v = \frac{\tau_Q}{4}$, $z = \frac{t}{\sqrt{\tau_Q}}$. By combining this observation with $\eta = 1/2$ version of Eq. (A18) one gets

$$|\Psi(t)\rangle = i\left[2\partial_t + \frac{t}{\tau_Q}\right][aD_{-\nu-1}(iz) + bD_{-\nu-1}(-iz)]|1\rangle$$
$$+ [aD_{-\nu-1}(iz) + bD_{-\nu-1}(-iz)]|2\rangle. \quad \text{(B10)}$$

Then the constants a and b from Eq. (B10) turn out to be equal to

$$a = \frac{1}{c}(\sqrt{\tau_Q}D_{-\nu-1}(iz_i)c_1(t_i) - 2D_{-\nu}(iz_i)c_2(t_i)),$$

$$b = \frac{1}{c}(\sqrt{\tau_Q}D_{-\nu-1}(-z_i)c_1(t_i) + 2D_{-\nu}(-iz_i)c_2(t_i)). \quad \text{(B11)}$$

where $c = 2D_{-\nu-1}(iz_i)D_{-\nu}(-iz_i) + 2D_{-\nu-1}(-iz_i)D_{-\nu}(iz_i)$.

(iii) *Exact solution of LZ when evolution begins from a ground state at* $t_i \to arccosh(\theta_0)\tau_Q$. When $\theta_0 = 0.2\pi$,

the initial state is $|\Psi(0)\rangle = (i/\sqrt{1 + e^{\frac{2\pi}{5}}}, 1/\sqrt{1 + e^{-\frac{2\pi}{5}}})$. The variables a and b from Eq. (B11) are proved to be equal to

$$a = \sqrt{\frac{\pi}{2}}\left(-\frac{i(\sqrt{11} + 6)}{20}\sqrt{\tau_Q} + \frac{25 - 3(\sqrt{11} + 3)}{25\sqrt{2\pi}}\tau_Q\right),$$

$$b = \sqrt{\frac{\pi}{2}}\left(-\frac{i(\sqrt{11} + 6)}{20}\sqrt{\tau_Q} - \frac{25 - 3(\sqrt{11} + 3)}{25\sqrt{2\pi}}\tau_Q\right). \quad \text{(B12)}$$

As a result, this straightforward calculation directly leads to Eq. (A15).

(iv) *Exact solution to the LZ problem when the evolution begins from a PT-symmetry broken ground state.* From $t_i \to -\infty$ to $t_f \to -t_n$. The initial state is $|\Psi(0)\rangle = |1^R\rangle$. Combining the initial condition $c_1(t_i)$, $c_2(t_i)$ and Eq. (B10), the constants a and b can be obtained

$$a = 0, \quad b = \frac{e^{-\frac{3}{8}i\pi\tau_Q}\tau_Q^{\frac{\tau_Q}{8}}\Gamma\left(\frac{\tau_Q}{4} + 1\right)}{\sqrt{2\pi}}. \quad \text{(B13)}$$

However, due to the nonunitary evolution, the time must be truncated, and assuming $t_i \to -\cosh(\frac{5\pi}{4}\tau_Q)$, density as a function of τ_Q is shown in Fig. 3. The relative occupation is equal to (A19).

---

[1] C. Zener, Non-adiabatic crossing of energy levels, Proc. R. Soc. London A **137**, 696 (1932).

[2] W. Wernsdorfer and R. Sessoli, Quantum phase interference and parity effects in magnetic molecular clusters, Science **284**, 133 (1999).

[3] W. Wernsdorfer, D. Mailly, and A. Benoit, Single nanoparticle measurement techniques, J. Appl. Phys. **87**, 5094 (2000).

[4] I. I. Rabi, Space quantization in a gyrating magnetic field, Phys. Rev. **51**, 652 (1937).

[5] E. Farhi, J. Goldstone, S. Gutmann, J. Lapan, A. Lundgren, and D. Preda, A quantum adiabatic evolution algorithm applied to random instances of an NP-complete problem, Science **292**, 472 (2001).

[6] A. M. Childs, E. Farhi, and J. Preskill, Robustness of adiabatic quantum computation, Phys. Rev. A **65**, 012322 (2001).

[7] N. Bender, H. Li, F. M. Ellis, and T. Kottos, Wave-packet self-imaging and giant recombinations via stable Bloch-Zener oscillations in photonic lattices with local $\mathcal{PT}$ symmetry, Phys. Rev. A **92**, 041803(R) (2015).

[8] M. Wimmer, M.-A. Miri, D. Christodoulides, and U. Peschel, Observation of Bloch oscillations in complex PT-symmetric photonic lattices, Sci. Rep. **5**, 17760 (2015).

[9] S. Xia, C. Danieli, Y. Zhang, X. Zhao, H. Lu, L. Tang, D. Li, D. Song, and Z. Chen, Higher-order exceptional point and Landau-Zener Bloch oscillations in driven non-Hermitian photonic Lieb lattices, APL Photonics **6**, 126106 (2021).

[10] R. El-Ganainy, K. G. Makris, M. Khajavikhan, Z. H. Musslimani, S. Rotter, and D. N. Christodoulides, Non-Hermitian physics and PT symmetry, Nat. Phys. **14**, 11 (2018).

[11] I. Rotter and J. P. Bird, A review of progress in the physics of open quantum systems: Theory and experiment, Rep. Prog. Phys. **78**, 114001 (2015).

[12] C. M. Bender and S. Boettcher, Real Spectra in Non-Hermitian Hamiltonians Having $\mathcal{PT}$ Symmetry, Phys. Rev. Lett. **80**, 5243 (1998).

[13] M. V. Berry, Physics of nonhermitian degeneracies, Czech. J. Phys. **54**, 1039 (2004).

[14] W.-Y. Wang and J. Liu, Adiabaticity of nonreciprocal Landau-Zener tunneling, Phys. Rev. A **106**, 063708 (2022).

[15] T. E. Lee, U. Alvarez-Rodriguez, X.-H. Cheng, L. Lamata, and E. Solano, Tachyon physics with trapped ions, Phys. Rev. A **92**, 032129 (2015).

[16] J. M. Zeuner, M. C. Rechtsman, Y. Plotnik, Y. Lumer, S. Nolte, M. S. Rudner, M. Segev, and A. Szameit, Observation of a Topological Transition in the Bulk of a Non-Hermitian System, Phys. Rev. Lett. **115**, 040402 (2015).

[17] T. Gao, E. Estrecho, K. Y. Bliokh, T. C. H. Liew, M. D. Fraser, S. Brodbeck, M. Kamp, C. Schneider, S. Höfling, Y. Yamamoto *et al.*, Observation of non-Hermitian degeneracies in a chaotic exciton-polariton billiard, Nature (London) **526**, 554 (2015).

[18] K. Kawabata, Y. Ashida, and M. Ueda, Information Retrieval and Criticality in Parity-Time-Symmetric Systems, Phys. Rev. Lett. **119**, 190401 (2017).

[19] L. Xiao, K. Wang, X. Zhan, Z. Bian, K. Kawabata, M. Ueda, W. Yi, and P. Xue, Observation of Critical Phenomena in Parity-Time-Symmetric Quantum Dynamics, Phys. Rev. Lett. **123**, 230401 (2019).

[20] R. Resta, Quantum-Mechanical Position Operator in Extended Systems, Phys. Rev. Lett. **80**, 1800 (1998).

[21] K. G. Makris, R. El-Ganainy, D. N. Christodoulides, and Z. H. Musslimani, Beam Dynamics in $\mathcal{PT}$ Symmetric Optical Lattices, Phys. Rev. Lett. **100**, 103904 (2008).

[22] R. El-Ganainy, K. G. Makris, D. N. Christodoulides, and Z. H. Musslimani, Theory of coupled optical PT-symmetric structures, Opt. Lett. **32**, 2632 (2007).

[23] Z. H. Musslimani, K. G. Makris, R. El-Ganainy, and D. N. Christodoulides, Optical Solitons in $\mathcal{PT}$ Periodic Potentials, Phys. Rev. Lett. **100**, 030402 (2008).

[24] A. Guo, G. J. Salamo, D. Duchesne, R. Morandotti, M. Volatier-Ravat, V. Aimez, G. A. Siviloglou, and D. N. Christodoulides, Observation of $\mathcal{PT}$-Symmetry Breaking in Complex Optical Potentials, Phys. Rev. Lett. **103**, 093902 (2009).

[25] C. E. Rüter, K. G. Makris, R. El-Ganainy, D. N. Christodoulides, M. Segev, and D. Kip, Observation of parity–time symmetry in optics, Nat. Phys. **6**, 192 (2010).

[26] W. D. Heiss, The physics of exceptional points, J. Phys. A: Math. Theor. **45**, 444016 (2012).

[27] B. Dóra, M. Heyl, and R. Moessner, The Kibble-Zurek mechanism at exceptional points, Nat. Commun. **10**, 2254 (2019).

[28] L. Xiao, D. Qu, K. Wang, H.-W. Li, J.-Y. Dai, B. Dóra, M. Heyl, R. Moessner, W. Yi, and P. Xue, Non-Hermitian kibble-zurek mechanism with tunable complexity in single-photon interferometry, PRX Quantum **2**, 020313 (2021).

[29] S. Yao and Z. Wang, Edge States and Topological Invariants of Non-Hermitian Systems, Phys. Rev. Lett. **121**, 086803 (2018).

[30] L. Xiao, T. Deng, K. Wang, Z. Wang, W. Yi, and P. Xue, Observation of Non-Bloch Parity-Time Symmetry and Exceptional Points, Phys. Rev. Lett. **126**, 230402 (2021).

[31] R. Hanai and P. B. Littlewood, Critical fluctuations at a many-body exceptional point, Phys. Rev. Res. **2**, 033018 (2020).

[32] J. Rogel-Salazar, Quantum Phase Transitions, 2nd edn., edited by S. Sachdev, Contemp. Phys. **53**, 77 (2012).

[33] L. Zhou, Qing-hai Wang, H. Wang, and J. Gong, Dynamical quantum phase transitions in non-Hermitian lattices, Phys. Rev. A **98**, 022129 (2018).

[34] S. Sachdev, *Quantum Phase Transitions* (Cambridge University Press, Cambridge, 2000).

[35] C. M. Bender, S. Boettcher, and P. N. Meisinger, PT-symmetric quantum mechanics, J. Math. Phys. **40**, 2201 (1999).

[36] C. M. Bender, D. C. Brody, and H. F. Jones, Complex Extension of Quantum Mechanics, Phys. Rev. Lett. **89**, 270401 (2002).

[37] G. Lévai and M. Znojil, Systematic search for PT-symmetric potentials with real energy spectra, J. Phys. A: Math. Gen. **33**, 7165 (2000).

[38] P. Silvi, G. Morigi, T. Calarco, and S. Montangero, Crossover from Classical to Quantum Kibble-Zurek Scaling, Phys. Rev. Lett. **116**, 225701 (2016).

[39] B. Gulácsi and B. Dóra, Defect production due to time-dependent coupling to environment in the Lindblad equation, Phys. Rev. B **103**, 205153 (2021).

[40] A. Zamora, G. Dagvadorj, P. Comaron, I. Carusotto, N. P. Proukakis, and M. H. Szymańska, Kibble-Zurek Mechanism in Driven Dissipative Systems Crossing a Nonequilibrium Phase Transition, Phys. Rev. Lett. **125**, 095301 (2020).

[41] S. Yin, G.-Y. Huang, C.-Y. Lo, and P. Chen, Kibble-Zurek Scaling in the Yang-Lee Edge Singularity, Phys. Rev. Lett. **118**, 065701 (2017).

[42] P. Nalbach, S. Vishveshwara, and A. A. Clerk, Quantum Kibble-Zurek physics in the presence of spatially correlated dissipation, Phys. Rev. B **92**, 014306 (2015).

[43] L. Henriet and K. Le Hur, Quantum sweeps, synchronization, and Kibble-Zurek physics in dissipative quantum spin systems, Phys. Rev. B **93**, 064411 (2016).

[44] P. Hedvall and J. Larson, Dynamics of non-equilibrium steady state quantum phase transitions, arXiv:1712.01560.

[45] B. Damski, The Simplest Quantum Model Supporting the Kibble-Zurek Mechanism of Topological Defect Production: Landau-Zener Transitions from a New Perspective, Phys. Rev. Lett. **95**, 035701 (2005).

[46] B. Damski and W. H. Zurek, Adiabatic-impulse approximation for avoided level crossings: From phase-transition dynamics to Landau-Zener evolutions and back again, Phys. Rev. A **73**, 063405 (2006).

[47] X.-Y. Xu, Y.-J. Han, K. Sun, J.-S. Xu, J.-S. Tang, C.-F. Li, and G.-C. Guo, Quantum Simulation of Landau-Zener Model Dynamics Supporting the Kibble-Zurek Mechanism, Phys. Rev. Lett. **112**, 035701 (2014).

[48] B. T. Torosov and N. V. Vitanov, Pseudo-Hermitian Landau-Zener-Stückelberg-Majorana model, Phys. Rev. A **96**, 013845 (2017).

[49] B. Longstaff and E.-M. Graefe, Nonadiabatic transitions through exceptional points in the band structure of a PT-symmetric lattice, Phys. Rev. A **100**, 052119 (2019).

[50] X. Shen, F. Wang, Z. Li, and Z. Wu, Landau-Zener-Stückelberg interferometry in $\mathcal{PT}$-symmetric non-Hermitian models, Phys. Rev. A **100**, 062514 (2019).

[51] Y. Avishai and Y. B. Band, Landau-Zener problem with decay and dephasing, Phys. Rev. A **90**, 032116 (2014).

[52] W. H. Zurek, U. Dorner, and P. Zoller, Dynamics of a Quantum Phase Transition, Phys. Rev. Lett. **95**, 105701 (2005).

[53] J. Dziarmaga, Dynamics of a quantum phase transition and relaxation to a steady state, Adv. Phys. **59**, 1063 (2010).

[54] J. Dziarmaga, Dynamics of a Quantum Phase Transition: Exact Solution of the Quantum Ising Model, Phys. Rev. Lett. **95**, 245701 (2005).

[55] X. Tong, Y.-M. Meng, X. Jiang, C. Lee, Gentil Dias de Moraes Neto, and G. Xianlong, Dynamics of a quantum phase transition in the Aubry-André-Harper model with p-wave superconductivity, Phys. Rev. B **103**, 104202 (2021).

[56] D. Sadhukhan, A. Sinha, A. Francuz, J. Stefaniak, M. M. Rams, J. Dziarmaga, and W. H. Zurek, Sonic horizons and causality in phase transition dynamics, Phys. Rev. B **101**, 144429 (2020).

[57] P. Laguna and W. H. Zurek, Density of Kinks after a Quench: When Symmetry Breaks, How Big are the Pieces? Phys. Rev. Lett. **78**, 2519 (1997).

[58] N. D. Antunes, L. M. A. Bettencourt, and W. H. Zurek, Vortex String Formation in a 3D U(1) Temperature Quench, Phys. Rev. Lett. **82**, 2824 (1999).

[59] F. Iglói, G. Roósz, and Y.-C. Lin, Non-equilibrium quench dynamics in quantum quasicrystals, New J. Phys. **15**, 023036 (2013).

[60] C. Bäuerle, Yu. M. Bunkov, S. N. Fisher, H. Godfrin, and G. R. Pickett, Laboratory simulation of cosmic string formation in the early Universe using superfluid 3He, Nature (London) **382**, 332 (1996).

[61] M. J. Bowick, L. Chandar, E. A. Schiff, and A. M. Srivastava, The cosmological Kibble mechanism in the laboratory: String formation in liquid crystals, Science **263**, 943 (1994).

[62] A. Maniv, E. Polturak, and G. Koren, Observation of Magnetic Flux Generated Spontaneously During a Rapid Quench of Superconducting Films, Phys. Rev. Lett. **91**, 197001 (2003).

[63] T. W. B. Kibble, Topology of cosmic domains and strings, J. Phys. A: Math. Gen. **9**, 1387 (1976).

[64] T. W. B. Kibble, Some implications of a cosmological phase transition, Phys. Rep. **67**, 183 (1980).

[65] W. H. Zurek, Cosmological experiments in superfluid helium? Nature (London) **317**, 505 (1985).

[66] W. H. Zurek, Cosmic strings in laboratory superfluids and the topological remnants of other phase transitions, Acta Phys. Polon. B **24**, 1301 (1993).

[67] W. H. Zurek, Cosmological experiments in condensed matter systems, Phys. Rep. **276**, 177 (1996).

[68] S. Ibáñez and J. G. Muga, Adiabaticity condition for non-Hermitian Hamiltonians, Phys. Rev. A **89**, 033403 (2014).

[69] G. Nenciu and G. Rasche, On the adiabatic theorem for nonself-adjoint Hamiltonians, J. Phys. A: Math. Gen. **25**, 5741 (1992).

[70] G. Dridi, S. Guérin, H. R. Jauslin, D. Viennot, and G. Jolicard, Adiabatic approximation for quantum dissipative systems: Formulation, topology, and superadiabatic tracking, Phys. Rev. A **82**, 022109 (2010).

[71] L.-J. Zhai, G.-Y. Huang, and S. Yin, Nonequilibrium dynamics of the localization-delocalization transition in the non-Hermitian Aubry-André model, Phys. Rev. B **106**, 014204 (2022).

[72] J. Wang, X.-J. Liu, G. Xianlong, and H. Hu, Phase diagram of a non-Abelian Aubry-André-Harper model with p-wave superfluidity, Phys. Rev. B **93**, 104504 (2016).

[73] Q. Lin, T. Li, L. Xiao, K. Wang, W. Yi, and P. Xue, Topological Phase Transitions and Mobility Edges in Non-Hermitian Quasicrystals, Phys. Rev. Lett. **129**, 113601 (2022).

[74] Y. Wang, L. Zhang, S. Niu, D. Yu, and X.-J. Liu, Realization and Detection of Nonergodic Critical Phases in an Optical Raman Lattice, Phys. Rev. Lett. **125**, 073204 (2020).

[75] A. Sinha, M. M. Rams, and J. Dziarmaga, Kibble-Zurek mechanism with a single particle: Dynamics of the localization-delocalization transition in the Aubry-André model, Phys. Rev. B **99**, 094203 (2019).